Numerical study of a two-dimensional problem in a constrained minimization theory of elasticity

Adair R. Aguiar[1], Lucas A. Rocha[1]

[1]*Department of Structural Engineering, São Carlos School of Engineering, University of São Paulo*
Av. Trabalhador Sãocarlense, 400, Cx. P. 359, 13560-590, São Carlos - SP - Brazil
aguiarar@sc.usp.br, lucas.almeida.rocha@usp.br

Abstract. We consider the equilibrium of a cylindrically orthotropic disk subject to a prescribed displacement on its boundary. In the context of classical linear elasticity, this problem has a solution that predicts material interpenetration. To prevent this unphysical behavior, we minimize the energy functional of classical linear elasticity subject to the local injectivity constraint. In previous work, we have obtained computational results showing that this problem has a rotationally symmetric solution that bifurcates from a radially symmetric solution. This secondary solution differs from a secondary solution reported in the literature, which was obtained by making no assumptions about the symmetry of the solution. Here, we extend the investigation of our previous work by making no a priori assumption on the symmetry of the displacement field. Using two different formulations, we obtain sequences of numerical solutions that converge to the rotationally symmetric solution mentioned above as the mesh is refined. In addition, there is no evidence of the existence of a third solution, which indicates that the rotationally symmetric solution is the only possible secondary solution. This research is of interest in the investigation of solids with radial microstructure, such as carbon fibers and certain types of wood.

Keywords: Orthotropy, Elasticity, Constrained minimization, Penalty method, Finite element method

1 Introduction

Some problems in the classical linear elasticity have solutions that predict the existence of regions where the material intersects itself. Of course, material interpenetration is not physically admissible. Locally, it is represented by non-positive values of the determinant of the deformation gradient. A possible way to prevent this behavior is to impose the local injectivity constraint, that is, the positiveness of the determinant of the deformation gradient.

In this work, we consider the equilibrium problem without body forces of a cylindrically orthotropic disk subject to a prescribed displacement on its boundary. In the context of the classical linear elasticity, Lekhnitskii [1] has obtained a closed form solution and shown that the radial and tangential stresses are singular at the center of the disk when the elastic modulus in the radial direction is greater than the elastic modulus in the tangential direction. Material properties of this type are found in carbon fibers with radial microstructure and certain types of wood; see, for instance, the works of Christensen [2] and Forest Products Laboratory [3]. For this class of materials, Fosdick and Royer-Carfagni [4] have shown that, in addition to singular stresses, the solution of the classical linear elasticity also predicts material interpenetration. To prevent this behavior, the authors have proposed a constrained minimization theory, in the context of which we minimize the energy functional of the classical linear elasticity subject to the local injectivity constraint. The authors have obtained a closed-form solution that does not predict material overlapping and is *radially symmetric*, in the sense that the displacement field has only the radial component and depends only on the radius.

The local injectivity constraint is nonlinear and, in general, the corresponding constrained minimization problem requires a numerical solution. Aguiar [5] has proposed a numerical procedure based on an interior penalty formulation and standard nonlinear programming techniques to solve a similar constrained minimization problem. Fosdick et al. [6] have used the numerical procedure of Aguiar [5] to obtain a secondary solution for the disk problem in the context of the constrained minimization theory. The authors have searched for a two-dimensional displacement field making no assumptions of symmetry.

Recently, Aguiar and Rocha [7] have revisited the constrained disk problem and searched for a solution that is *rotationally symmetric*, in the sense that the radial and tangential components depend only on the radius. The authors have obtained numerical results that converge to a solution that is different from the solution of Fosdick et al. [6]. In particular, in the rotationally symmetric solution, the tangential displacement is linear in a neighborhood of the center of the disk. In addition, to obtain the rotationally symmetric solution, the authors have had to introduce a perturbation in the initial guess used in the numerical procedure for, otherwise, only the radially symmetric solution was obtained.

In this work we search for a solution of the constrained disk problem making no assumptions about its symmetry. We use two different formulations, namely the *polar* and the *Cartesian* formulations. The former represents all fields in terms of the polar coordinates and is a natural extension of the formulation used by Aguiar and Rocha [7]. The latter represents all fields in terms of the Cartesian coordinates. The Cartesian formulation is similar to the formulation used by Fosdick et al. [6] and is included here for comparison purposes. Using both formulations, we obtain convergent sequences of numerical solutions that converge to the rotationally symmetric solution of Aguiar and Rocha [7]. These results indicate that the rotationally symmetric solution is the only possible secondary solution of the constrained disk problem.

In Section 2, we present the constrained disk problem together with its polar and Cartesian formulations. We then review the numerical procedure of Aguiar [5] that is used to obtain the numerical solutions for the corresponding constrained minimization problems. In Section 3, we present the numerical results, which indicate that the numerical solutions tend to the rotationally symmetric solution of Aguiar and Rocha [7] as the meshes used in the finite element approximations are refined. In Section 4, we present some concluding remarks.

2 The disk problem

Let $\mathcal{B} \subset \mathbb{R}^2$ be the undistorted natural reference configuration of a solid. Points $\mathbf{X} \in \mathcal{B}$ are mapped to points $\mathbf{x} := \mathbf{f}(\mathbf{X}) = \mathbf{X} + \mathbf{u}(\mathbf{X})$, $\mathbf{x} \in \mathbb{R}^2$, where $\mathbf{u}(\mathbf{X})$ is the displacement of $\mathbf{X}$. The boundary $\partial\mathcal{B}$ of $\mathcal{B}$ is composed of two non-intersecting parts, $\partial_1\mathcal{B}$ and $\partial_2\mathcal{B}$, $\partial\mathcal{B} = \partial_1\mathcal{B} \cup \partial_2\mathcal{B}$, $\partial_1\mathcal{B} \cap \partial_2\mathcal{B} = \emptyset$, such that $\mathbf{u}(\mathbf{X}) = \bar{\mathbf{u}}(\mathbf{X})$ for $\mathbf{X} \in \partial_1\mathcal{B}$, where $\bar{\mathbf{u}}$ is a known vector-valued function, and a dead load traction field $\bar{\mathbf{t}}(\mathbf{X})$ is prescribed for $\mathbf{X} \in \partial_2\mathcal{B}$. In addition, a body force $\mathbf{b}(\mathbf{X})$ per unit of volume acts on $\mathbf{X} \in \mathcal{B}$.

We consider the problem of minimization of the total potential energy of classical linear elasticity, given by

$$\min_{\mathbf{u}\in\mathcal{A}_\varepsilon} \mathcal{E}[\mathbf{u}]\,, \qquad \mathcal{E}[\mathbf{u}] = \frac{1}{2}\int_{\mathcal{B}} \mathbb{C}[\mathbf{E}] \cdot \mathbf{E}\, d\mathbf{X} - \int_{\mathcal{B}} \mathbf{b}\cdot\mathbf{u}\, d\mathbf{X} - \int_{\partial_2\mathcal{B}} \bar{\mathbf{t}}\cdot\mathbf{u}\, d\mathbf{X}\,, \tag{1}$$

where

$$\mathcal{A}_\varepsilon := \left\{\mathbf{u} \in \mathcal{W}^{1,2}(\mathcal{B}) \to \mathbb{R}^2 \mid \det(\mathbf{1}+\nabla\mathbf{u}) \geq \varepsilon > 0,\ \mathbf{u} = \bar{\mathbf{u}} \text{ on } \partial_1\mathcal{B}\right\} \tag{2}$$

is the set of kinematically admissible displacements with ε being a sufficiently small positive parameter. Furthermore, $\mathbf{E}$ is the infinitesimal strain tensor and $\mathbb{C}$ is the elasticity tensor, which is symmetric and positive definite. If the injectivity constraint $\det(\mathbf{1}+\nabla\mathbf{u}) \geq \varepsilon > 0$ were not present, the constrained minimization problem stated above would become the minimization problem of classical linear elasticity theory.

Let $\mathcal{B} = \mathcal{B}_> \cup \mathcal{B}_=$, $\mathcal{B}_> \cap \mathcal{B}_= = \emptyset$, where

$$\mathcal{B}_> := \mathrm{int}[\{\mathbf{X} \in \mathcal{B} \mid \det\nabla\mathbf{f}(\mathbf{X}) > \varepsilon\}]\,, \qquad \mathcal{B}_= := \mathrm{int}[\{\mathbf{X} \in \mathcal{B} \mid \det\nabla\mathbf{f}(\mathbf{X}) = \varepsilon\}]\,, \tag{3}$$

and $\mathrm{int}[\cdot]$ denotes the interior of a set. Fosdick and Royer-Carfagni [4] have shown that the Euler-Lagrange equations for the constrained minimization problem defined by eq. (1) and eq. (2) are given by

$$\mathrm{Div}\,\mathbf{T} + \mathbf{b} = \mathbf{0} \quad \text{in } \mathcal{B}_>\,, \qquad \mathrm{Div}\,(\mathbf{T} - \varepsilon\lambda(\nabla\mathbf{f})^{-T}) + \mathbf{b} = \mathbf{0} \quad \text{in } \mathcal{B}_=\,, \tag{4}$$

where $\lambda(\mathbf{X}) \geq 0$ is the Lagrange multiplier field associated with the injectivity constraint $\det(\mathbf{1}+\nabla\mathbf{u}) \geq \varepsilon > 0$ and $\mathbf{T} = \mathbb{C}[\mathbf{E}]$ is the stress tensor. The boundary conditions are given by

$$\mathbf{T}\,\mathbf{n} = \bar{\mathbf{t}} \quad \text{in } \partial_2\mathcal{B}_>\,, \qquad (\mathbf{T} - \varepsilon\lambda(\nabla\mathbf{f})^{-T})\,\mathbf{n} = \bar{\mathbf{t}} \quad \text{in } \partial_2\mathcal{B}_=\,, \tag{5}$$

where $\mathbf{n}$ is a unit normal to $\partial_2\mathcal{B}$. In addition, the jump condition

$$(\mathbf{T} - \varepsilon\lambda(\nabla\mathbf{f})^{-T})|_{\Sigma\cap\bar{\mathcal{B}}_=}\,\mathbf{n} = \mathbf{T}|_{\Sigma\cap\bar{\mathcal{B}}_>}\,\mathbf{n} \tag{6}$$

must hold across $\Sigma := \bar{\mathcal{B}}_> \cap \bar{\mathcal{B}}_=$, where $\mathbf{n}$ is a unit normal to Σ and where $\Sigma \cap \bar{\mathcal{B}}_=$ and $\Sigma \cap \bar{\mathcal{B}}_>$ mean that the evaluations are understood as limits to the dividing interface Σ from within $\mathcal{B}_=$ and $\mathcal{B}_>$, respectively.

In the interior penalty formulation of Aguiar [5], we replace the energy functional of eq. (1.b) by a penalized potential energy functional $\mathcal{E}_\delta : \mathcal{A}_\varepsilon \to \mathbb{R}$ defined by

$$\mathcal{E}_\delta[\mathbf{u}] := \mathcal{E}[\mathbf{u}] + \mathcal{P}[\mathbf{u}] \,/\, \delta \,, \tag{7}$$

where $\delta > 0$ is a penalty parameter and $\mathcal{P}[\mathbf{u}] : \mathcal{A}_\varepsilon \to \mathbb{R}$ is a barrier functional, which must satisfy $\mathcal{P}[\mathbf{u}] > 0, \forall\, \mathbf{u} \in \mathcal{A}_\varepsilon$, and $\mathcal{P}[\mathbf{u}] \to \infty$ as $\mathbf{u}$ approaches the boundary of $\mathcal{A}_\varepsilon$. The addition of the term $\mathcal{P}/\delta$ establishes a barrier on the boundary of the constraint set $\mathcal{A}_\varepsilon$ that prevents the minimizing procedure from leaving the set $\mathcal{A}_\varepsilon$. We then solve a sequence of minimization problems of the form

$$\min_{\mathbf{u} \in \mathcal{A}_\varepsilon} \mathcal{E}_\delta[\mathbf{u}] \tag{8}$$

for increasingly larger values of δ. In the limit as $\delta \to \infty$, the solution of the penalized minimization problem given by eq. (8) tends to the solution of the original minimization problem given by eq. (1). We use the same barrier functional $\mathcal{P}[\mathbf{u}]$ used by Aguiar [5] and Fosdick et al. [6], which is given by

$$\mathcal{P}[\mathbf{u}] := \int_{\mathcal{B}} \left[\det(\mathbf{1} + \nabla \mathbf{u}) - \varepsilon\right]^{-1} \, d\mathbf{X} \,, \qquad \forall \mathbf{u} \in \mathcal{A}_\varepsilon \,. \tag{9}$$

In this work, we consider that $\mathcal{B}$ is a circular disk of radius R_e with its center at the origin of the coordinate system. There is no body force, $\mathbf{b} = \mathbf{0}$, and the disk is subject to a prescribed radial displacement $\bar{\mathbf{u}} = \bar{u}_r \, \mathbf{e}_r$ on its entire boundary, that is, $\partial\mathcal{B} = \partial_1\mathcal{B}$ and $\partial_2\mathcal{B} = \emptyset$. We express the energy and barrier functionals, given by eq. (1.b) and eq. (9), respectively, with both a polar coordinate system (R, Θ) with the associated orthonormal basis $\{\mathbf{e}_r, \mathbf{e}_\theta\}$ and a Cartesian coordinate system (X_1, X_2) with the associated orthonormal basis $\{\mathbf{e}_1, \mathbf{e}_2\}$. The former takes advantage of the geometry of the disk, the radial application of the load, and the material properties. The latter is included for comparison purposes with the work of Fosdick et al. [6]. In addition, we assume that the disk is composed of a cylindrically orthotropic material, in the sense that the components of $\mathbb{C}$ are constant relative to the basis $\{\mathbf{e}_r, \mathbf{e}_\theta\}$.

We make no assumptions about the symmetry of the displacement field. Thus, relative to the basis $\{\mathbf{e}_r, \mathbf{e}_\theta\}$, it has the form

$$\mathbf{u}(R, \Theta) = u_r(R, \Theta) \, \mathbf{e}_r + u_\theta(R, \Theta) \, \mathbf{e}_\theta \,. \tag{10}$$

From the Generalized Hooke's Law, $\mathbf{T} = \mathbb{C}[\mathbf{E}]$, the components of the stress and strain tensors in, respectively,

$$\mathbf{T} = \sigma_{rr} \, \mathbf{e}_r \otimes \mathbf{e}_r + \sigma_{\theta\theta} \, \mathbf{e}_\theta \otimes \mathbf{e}_\theta + \sigma_{r\theta} \left(\mathbf{e}_r \otimes \mathbf{e}_\theta + \mathbf{e}_\theta \otimes \mathbf{e}_r\right), \tag{11}$$

$$\mathbf{E} = \epsilon_{rr} \, \mathbf{e}_r \otimes \mathbf{e}_r + \epsilon_{\theta\theta} \, \mathbf{e}_\theta \otimes \mathbf{e}_\theta + \epsilon_{r\theta} \left(\mathbf{e}_r \otimes \mathbf{e}_\theta + \mathbf{e}_\theta \otimes \mathbf{e}_r\right) \tag{12}$$

are related to each other by

$$\sigma_{rr} = c_{11} \, \epsilon_{rr} + c_{12} \, \epsilon_{\theta\theta} \,, \qquad \sigma_{\theta\theta} = c_{12} \, \epsilon_{rr} + c_{22} \, \epsilon_{\theta\theta} \,, \qquad \sigma_{r\theta} = 2 \, c_{66} \, \epsilon_{r\theta} \,, \tag{13}$$

where the constants c_{11}, c_{22}, c_{12}, c_{66} are the components of $\mathbb{C}$ relative to the basis $\{\mathbf{e}_r, \mathbf{e}_\theta\}$ and

$$\epsilon_{rr} = u_{r,R} \,, \qquad \epsilon_{\theta\theta} = \frac{u_r}{R} + \frac{u_{\theta,\Theta}}{R} \,, \qquad \epsilon_{r\theta} = \frac{1}{2}\left(\frac{u_{r,\Theta}}{R} + u_{\theta,R} - \frac{u_\theta}{R}\right), \tag{14}$$

with $(\cdot)_{,A}$ denoting the partial derivative $\partial(\cdot)/\partial A$.

It follows from eq. (10)-(14) that the energy functional $\mathcal{E}$, given by eq. (1.b), and the barrier functional $\mathcal{P}$, given by eq. (9), can be written as, respectively,

$$\begin{aligned} \mathcal{E}[\mathbf{u}] = \int_0^{2\pi}\!\!\int_0^{R_e} \Bigg(& \frac{c_{11} \, R \, u_{r,R}^2}{2} + c_{12} \, u_r \, u_{r,R} + c_{12} \, u_{r,R} \, u_{\theta,\Theta} + \frac{c_{22} \, u_r^2}{2R} + \frac{c_{22} \, u_r \, u_{\theta,\Theta}}{R} + \frac{c_{22} \, u_{\theta,\Theta}^2}{2R} + \\ & \frac{c_{66} \, R \, u_{\theta,R}^2}{2} - c_{66} \, u_\theta \, u_{\theta,R} + c_{66} \, u_{r,\Theta} \, u_{\theta,R} + \frac{c_{66} \, u_\theta^2}{2R} - \frac{c_{66} \, u_\theta \, u_{r,\Theta}}{R} + \frac{c_{66} \, u_{r,\Theta}^2}{2R} \Bigg) dR \, d\Theta \,, \end{aligned} \tag{15}$$

$$\mathcal{P}[\mathbf{u}] = \int_0^{2\pi}\!\!\int_0^{R_e} \frac{R \, dR \, d\Theta}{(1 + u_{r,R})\,(1 + u_r/R + u_{\theta,\Theta}/R) - u_{\theta,R}\,(u_{r,\Theta}/R - u_\theta/R) - \varepsilon} \,. \tag{16}$$

The constrained minimization problem given by eq. (8) together with eq. (7), eq. (15) and eq. (16) is referred to as the *polar formulation*.

To obtain the Cartesian formulation, we first note that the elasticity tensor $\mathbb{C}$ is not constant relative to the basis $\{\mathbf{e}_1, \mathbf{e}_2\}$. In fact, its components are given by

$$c^c_{ijkl}(\mathbf{X}) = Q_{mi}\, Q_{nj}\, Q_{ok}\, Q_{pl}\, c_{mnop}\,, \tag{17}$$

with $i, j, k, l = 1, 2$ and implicit sum from 1 to 2 over the repeated indices. In eq. (17), we use the rules $11 \to 1$, $22 \to 2$, and $12 \to 6$ to see that c_{mnop} represent the constants c_{11}, c_{12}, c_{22}, and c_{66} of eq. (13). In addition, Q_{ij} are the components of the transformation matrix

$$\mathbf{Q} = [Q_{ij}] = \begin{bmatrix} \cos\Theta & \sin\Theta \\ -\sin\Theta & \cos\Theta \end{bmatrix}, \tag{18}$$

where Θ is the polar angle of the material point $\mathbf{X} = X_i\, \mathbf{e}_i$ and is given by $\Theta = \arctan(X_2/X_1)$. In addition, the displacement field has the form

$$\mathbf{u}(\mathbf{X}) = u_1(X_1, X_2)\, \mathbf{e}_1 + u_2(X_1, X_2)\, \mathbf{e}_2\,. \tag{19}$$

Similar to the steps that lead to eq. (15) and eq. (16), we obtain that the energy functional $\mathcal{E}$, given by eq. (1.b), and the barrier functional $\mathcal{P}$, given by eq. (9), can be written as, respectively,

$$\begin{aligned} \mathcal{E}[\mathbf{u}] = \int_{\mathcal{B}} \Bigg(& \frac{c^c_{11}\, u^2_{1,1}}{2} + c^c_{12}\, u_{1,1}\, u_{2,2} + c^c_{16}\, u_{1,1}\, u_{1,2} + c^c_{16}\, u_{1,1}\, u_{2,1} + \frac{c^c_{22}\, u^2_{2,2}}{2} \\ & + c^c_{26}\, u_{1,2}\, u_{2,2} + c^c_{26}\, u_{2,1}\, u_{2,2} + c^c_{66} \frac{u^2_{1,2}}{2} + c^c_{66}\, u_{1,2}\, u_{2,1} + \frac{c^c_{66}\, u^2_{2,1}}{2} \Bigg) d\mathbf{X}\,, \end{aligned} \tag{20}$$

$$\mathcal{P}[\mathbf{u}] = \int_{\mathcal{B}} \frac{1}{(1 + u_{1,1})(1 + u_{2,2}) - u_{1,2}\, u_{2,1} - \varepsilon}\, d\mathbf{X}\,, \tag{21}$$

where, again, we use the rules $11 \to 1$, $22 \to 2$, and $12 \to 6$ to represent the elastic constants, and we omit their dependence on $\mathbf{X}$. The constrained minimization problem given by eq. (8) together with eq. (7), eq. (20) and eq. (21) is referred to as the *Cartesian formulation*.

Next, we present the discrete versions of the polar and Cartesian formulations. Let $\mathcal{V}_h$ be a finite element space spanned by a set of vector-valued basis functions $\{\mathbf{w}_i\}$, where h stands for the characteristic length of the finite element. A finite element approximation $\mathbf{u}_h \in \mathcal{V}_h$ for the penalized minimization problem, given by eq. (8), can be written as

$$\mathbf{u}_h = \sum_{i=1}^{m} s^i\, \mathbf{w}_i\,, \tag{22}$$

where $s^i \in \mathbb{R}$, $i = 1, 2, ..., m$, is a degree of freedom and m is the number of degrees of freedom associated with the discretization. We introduce the vector of degrees of freedom $\mathbf{s} := (s^1, s^2, ..., s^m)$ and the functions $\mathcal{E}_h(\mathbf{s}) := \mathcal{E}[\mathbf{u}_h]$ and $\mathcal{P}_h(\mathbf{s}) := \mathcal{P}[\mathbf{u}_h]$. Then, the discrete version of the penalized functional of eq. (7) is given by

$$\mathcal{F}_\delta(\mathbf{s}) := \mathcal{E}_h(\mathbf{s}) + \mathcal{P}_h(\mathbf{s}) \,/\, \delta \tag{23}$$

and the associated minimization problem is given by

$$\min_{\mathbf{s} \in \mathbb{R}^m} \mathcal{F}_\delta(\mathbf{s}) \tag{24}$$

subject to $\det(\mathbf{1} + \nabla \mathbf{u}) \geq \varepsilon > 0$ in parts of the domain where $\mathbf{u}_h$ is smooth.

We solve the minimization problem given by eq. (24) iteratively using the numerical procedure proposed by Aguiar [5], which is based on the Newton-Raphson method together with a line search. In summary, we start from an initial guess $\mathbf{s}_0$ and a penalty parameter δ. We generate a sequence of vectors $\mathbf{s}_k$, $k = 1, 2, 3, ...$, which converges to a solution $\mathbf{s}^\delta_h$ of the discrete minimization problem given by eq. (24). Then, we increase δ and repeat the previous procedure starting from $\mathbf{s}_0 = \mathbf{s}^\delta_h$. As $\delta \to \infty$, the sequence of solutions $\{\mathbf{s}^\delta_h\}$ converges to a vector $\mathbf{s}_h = (s^1, s^2, ..., s^m)$ that yields the approximate solution $\mathbf{u}_h \in \mathcal{V}_h$, given by eq. (22). By letting $h \to 0$, we generate a sequence of approximations $\{\mathbf{u}_h\}$ which converges to the minimizer of the original problem given by eq. (1).

3 Numerical results

In this section we apply the numerical procedure of Aguiar [5] with the formulation presented in Section 2 to obtain numerical solutions of the constrained disk problem. For comparison purposes, we use the same material

and geometric parameters used by Fosdick et al. [6] and Aguiar and Rocha [7], which are given, in dimensionless units, by $\bar{u}_r := \bar{\mathbf{u}} \cdot \mathbf{e}_r = -0.05$, $c_{11} = 10^5$, $c_{22} = 10^4$, $c_{12} = 10^3$, $c_{66} = 10^3$, $\varepsilon = 0.1$, and $R_e = 1$. In addition, the numerical results presented below correspond to $\delta = 10^8$; we have verified that the results do not change significantly for larger values of δ.

In the polar formulation, we use isoparametric bilinear finite elements defined on the domain $(0, R_e) \times (0, 2\,\pi)$ to construct the approximations $\mathbf{u}_h$ in eq. (22). We construct the mesh by dividing the interval $(0, R_e)$ in $600\,q$, $q \in \{1, 4, 16\}$, subintervals as follows: $375\,q$ elements in $(0, 0.07\,R_e)$, $125\,q$ elements in $(0.07\,R_e, 0.46\,R_e)$, and $100\,q$ elements in $(0.46\,R_e, R_e)$. The interval $(0, 2\,\pi)$ is divided uniformly in 64 subintervals. Therefore, the rectangular domain $(0, R_e) \times (0, 2\,\pi)$ is the union of $600\,q \times 64$ rectangles.

In the Cartesian formulation, we also use isoparametric bilinear finite elements. However, in this case, they are defined in a discrete domain $\mathcal{B}_h$, which approximates the circular domain $\mathcal{B}$. The discrete domain $\mathcal{B}_h$ is composed of $N = 2128, 7162$, or, 22448 quadrilateral elements with its boundary being discretized by $64, 128$, or, 256 segments of straight lines, respectively. In addition, in all three cases, the characteristic size of the elements at the center of $\mathcal{B}_h$ is 10^{-4}.

In the polar formulation, the components of $\mathbf{s} = (s^1, s^2, ..., s^m)$, with $m = 2\,M$ and M being the number of mesh nodes, are given by $s^{2\,i-1} := \mathbf{u}_h(R_i, \Theta_i) \cdot \mathbf{e}_r$ and $s^{2\,i} := \mathbf{u}_h(R_i, \Theta_i) \cdot \mathbf{e}_\theta$, where $i = 1, 2, ..., M$ and (R_i, Θ_i) are the polar coordinates of the *i*-th mesh node. To obtain a numerical solution that is different from the radially symmetric solution, we consider that the components with odd indices of the initial guess $\mathbf{s}_0$ are given by $s_0^{2\,i-1} = \bar{u}_r\,R_i/R_e$ for $i = 1, 2, ..., M$, and the components with even indices by $s_0^{2\,i} = u_\theta^0$ for $1 < i < M$, where u_θ^0 is a small perturbation, and $s_0^2 = s_0^{2\,M} = 0$. Here, we use $u_\theta^0 = 10^{-2}$. Different values of u_θ^0 do not affect much the numerical results, except if they are too small, in which case the numerical procedure converges only to the radially symmetric solution. The necessity of a large enough perturbation in the tangential displacement was also observed by Aguiar and Rocha [7].

In the Cartesian formulation, the components of $\mathbf{s} = (s^1, s^2, ..., s^m)$ are given by $s^{2\,i-1} := \mathbf{u}_h(X_1^i, X_2^i) \cdot \mathbf{e}_1$ and $s^{2\,i} := \mathbf{u}_h(X_1^i, X_2^i) \cdot \mathbf{e}_2$, where $i = 1, 2, ..., M$ and (X_1^i, X_2^i) are the Cartesian coordinates of the *i*-th mesh node. In this case, we use the solution of the isotropic disk problem, given by $\mathbf{u} = (R/R_e)\,\bar{\mathbf{u}}$, as the initial guess for the numerical procedure. There is no need to perturb the tangential displacement, because, for the considered meshes, the error introduced by the approximation of the circular boundary of the disk with straight line segments acts as a perturbation.

In Fig. 1, we show the radial displacement u_r versus the radius R. The solid lines represent u_r obtained with the polar formulation for $q = 1, 4, 16$, and the dashed line represents u_r of the rotationally symmetric solution from Aguiar and Rocha [7]. Fig. 1a refers to the entire interval $(0, R_e)$ and Fig. 1b refers to a neighborhood of the origin given by the interval $(0, 0.05)$. We see from both figures that the curves are very close to each other.

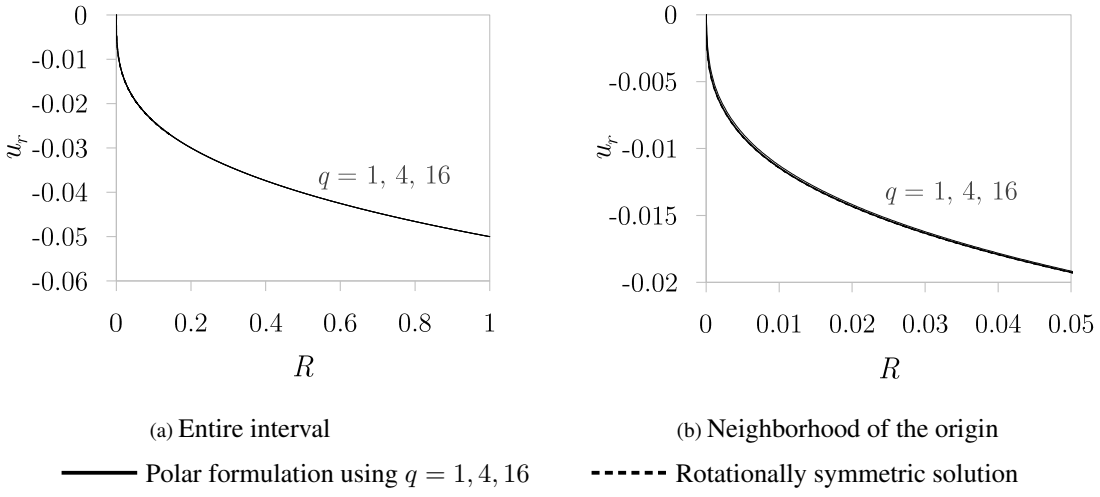

(a) Entire interval (b) Neighborhood of the origin

Polar formulation using $q = 1, 4, 16$ Rotationally symmetric solution

Figure 1. Radial displacement u_r versus the radius R. Polar formulation and rotationally symmetric solution of Aguiar and Rocha [7].

In Fig. 2, we show the tangential displacement u_θ versus the radius R. Similarly to Fig. 1, the solid lines represent u_θ obtained with the polar formulation for $q = 1, 4, 16$, and the dashed line represents u_θ of the rotationally symmetric solution from Aguiar and Rocha [7]. Again, the results are presented for $R \in (0, R_e)$ in Fig 2a and for $(0, 0.05)$ in Fig. 2b. We see from Fig. 2a that the curves are indistinguishable and, from Fig. 2b, that u_θ of the polar formulation tends to u_θ of the rotationally symmetric solution. In particular, u_θ tends to a linear

function in a neighborhood of the origin.

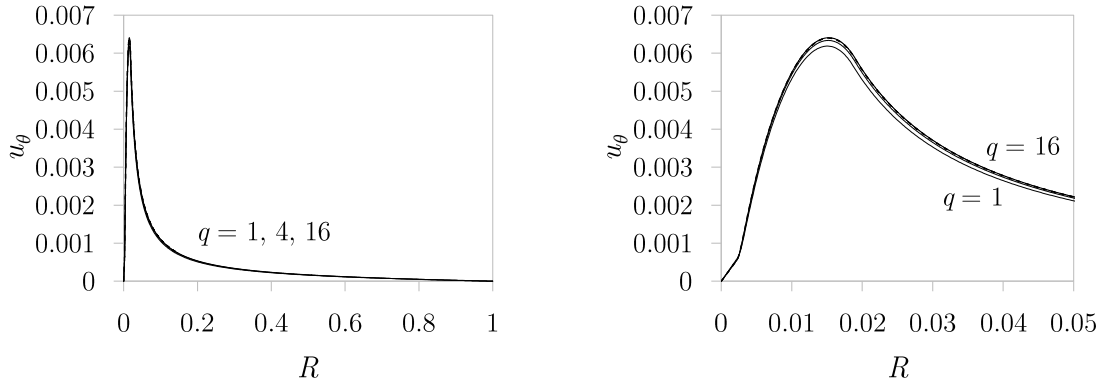

(a) Entire interval (b) Neighborhood of the origin

Polar formulation using $q = 1, 4, 16$ Rotationally symmetric solution

Figure 2. Tangential displacement u_θ versus the radius R. Polar formulation and rotationally symmetric solution of Aguiar and Rocha [7].

Next, to present the results of the Cartesian formulation, we consider $X_2 = 0$, which corresponds to $\Theta = 0$, and plot graphs of $u_r(R)$ and $u_\theta(R)$, where, here, $R = X_1 \in (0, R_e)$, $u_r(R) = u_1(X_1, 0)$, and $u_\theta(R) = u_2(X_1, 0)$. These graphs are shown in Fig. 3 and Fig 4, which correspond to, respectively, Fig. 1 and Fig. 2 obtained with the polar formulation. We see from Fig. 3 and Fig. 4 that, again, both u_r and u_θ of the Cartesian formulation tend to u_r and u_θ of the rotationally symmetric solution, respectively, as the mesh is refined.

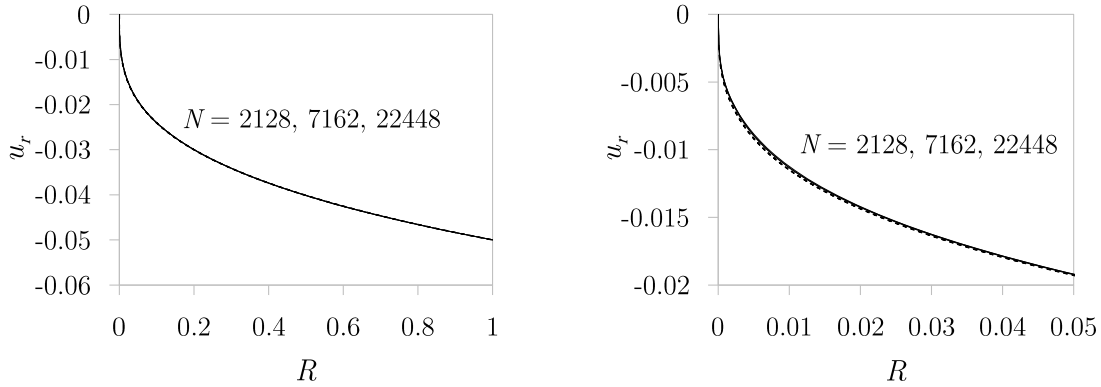

(a) Entire interval (b) Neighborhood of the origin

Cartesian formulation using $N = 2128, 7162, 22448$ Rotationally symmetric solution

Figure 3. Radial displacement u_r versus the radius R. Cartesian formulation and rotationally symmetric solution of Aguiar and Rocha [7].

In summary, by using both polar and Cartesian formulations, the numerical approximations converge to the rotationally symmetric solution of Aguiar and Rocha [7] and do not seem to depend on the polar angle Θ. In addition, there is no evidence of the existence of a third solution, which could, for instance, depend on Θ.

4 Conclusions

We have considered the problem of a cylindrically orthotropic disk in equilibrium with no body forces and subjected to a prescribed displacement on its boundary. We have searched for two-dimensional displacement fields, making no assumptions about their symmetries, in the context of a constrained minimization theory of elasticity that enforces the local injectivity constraint. We have formulated the problem in two different ways, which correspond to the polar and the Cartesian formulations. Below, we list the main results of this work.

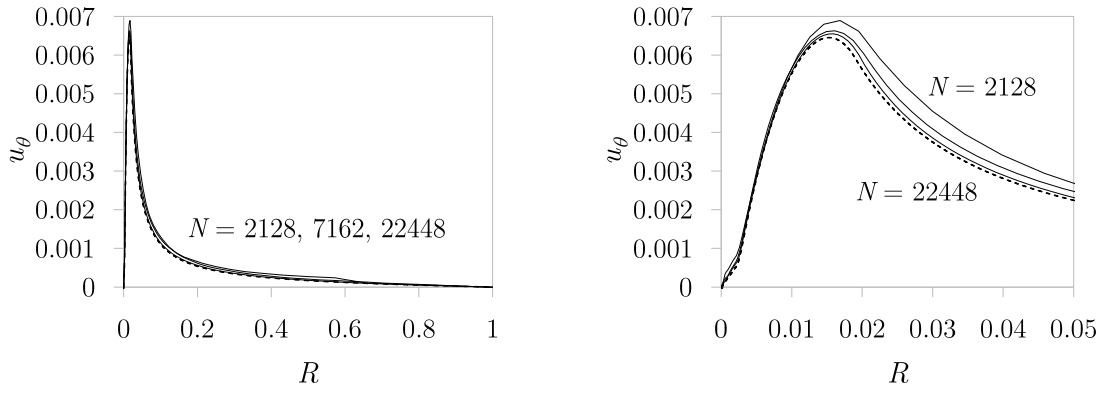

(a) Entire interval

(b) Neighborhood of the origin

Cartesian formulation using $N = 2128, 7162, 22448$

Rotationally symmetric solution

Figure 4. Tangential displacement u_θ versus the radius R. Cartesian formulation and rotationally symmetric solution of Aguiar and Rocha [7].

- Using the polar and the Cartesian formulations, we have obtained sequences of numerical results that converge to the rotationally symmetric solution reported by Aguiar and Rocha [7], which was obtained by assuming that the displacement field depends only on the radius. In particular, near the center of the disk, the tangential displacement is a linear function of the radius.
- In the polar formulation, to obtain a secondary solution that is different from the radially symmetric solution, we must perturb the tangential displacement of the initial guess used in the numerical procedure. In the Cartesian formulation, for the considered meshes, such an explicit perturbation is not required, because the error introduced by the approximation of the circular boundary with segments of straight lines introduces a perturbation in the tangential displacement.
- We have obtained no evidence of the existence of a third solution, which indicates that the rotationally symmetric solution of Aguiar and Rocha [7] is the only possible secondary solution for the orthotropic disk problem considered in this work.

Acknowledgements. The first author acknowledges the support of National Council for Scientific and Technological Development (CNPq), grant nº 420099/2018-2, and the second author acknowledges the financial support provided by Coordination for the Improvement of Higher Education Personnel (CAPES) - Finance Code 001.

Authorship statement. The authors hereby confirm that they are the sole liable persons responsible for the authorship of this work, and that all material that has been herein included as part of the present paper is either the property (and authorship) of the authors, or has the permission of the owners to be included here.

References

[1] S. G. Lekhnitskii. *Anisotropic plates*. Gordon & Breach, New York, 1968.
[2] R. M. Christensen. Properties of carbon fibers. *Journal of the Mechanics and Physics of Solids*, vol. 42, n. 4, pp. 681–695, 1994.
[3] Forest Products Laboratory. Wood handbook - Wood as an engineering material. Technical report, U.S. Department of Agriculture, Forest Service, Forest Products Laboratory, Madison, 2010.
[4] R. Fosdick and G. Royer-Carfagni. The constraint of local injectivity in linear elasticity theory. *Proceedings of the Royal Society A: Mathematical, Physical and Engineering Sciences*, vol. 457, n. 2013, pp. 2167–2187, 2001.
[5] A. R. Aguiar. Local and global injective solution of the rotationally symmetric sphere problem. *Journal of Elasticity*, vol. 84, n. 2, pp. 99–129, 2006.
[6] R. Fosdick, F. Freddi, and G. Royer-Carfagni. Bifurcation instability in linear elasticity with the constraint of local injectivity. *Journal of Elasticity*, vol. 90, n. 1, pp. 99–126, 2008.
[7] A. R. Aguiar and L. A. Rocha. Numerical investigation of bifurcation instability in constrained minimization problem of elasticity. In *Proceedings of the Ibero-Latin-American Congress on Computational Methods in Engineering*, 2020.